EPSRC
Engineering and Physical Sciences Research Council

InFoMM
Industrially Focused Mathematical Modelling

EPSRC Centre for Doctoral Training in Industrially Focused Mathematical Modelling

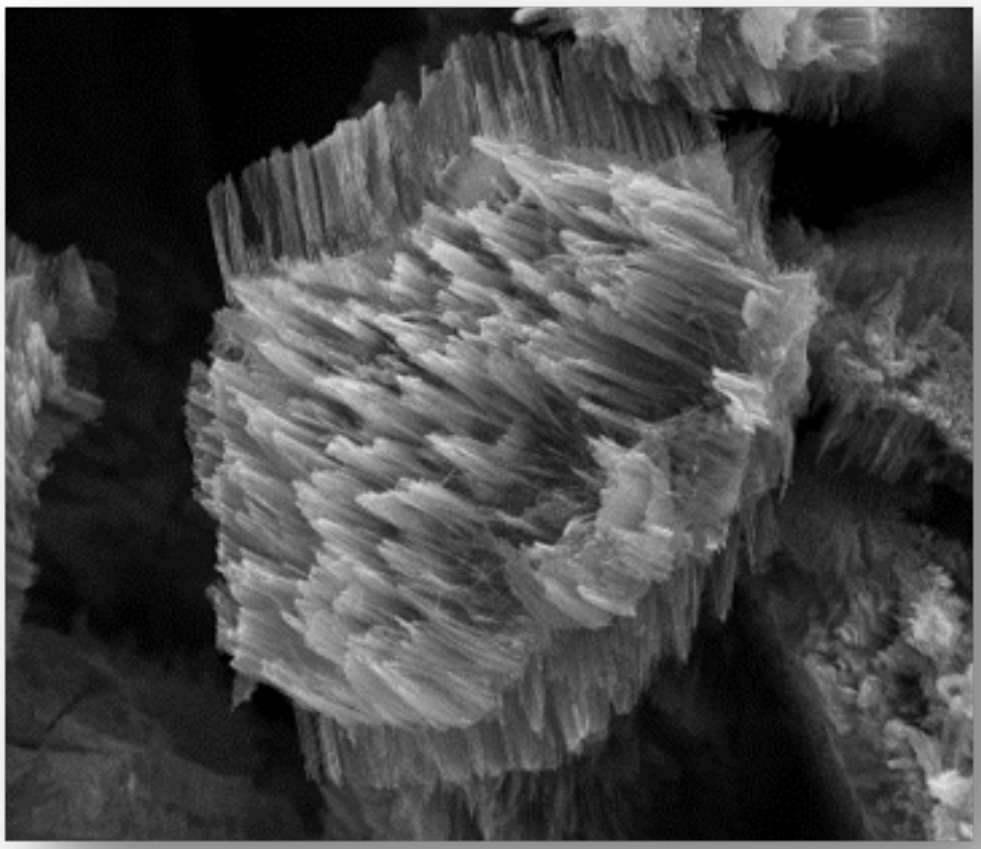

Silicon Anodes in Lithium-Ion Batteries

Ian Roper

UNIVERSITY OF OXFORD

nexeon®

Contents

1 Introduction

Lithium-Ion Batteries

Lithium-ion batteries (LIBs) are one of the leading technologies for energy storage. LIBs comprise one or more cells joined in series with each other to increase the voltage the battery produces. Each cell induces an electrical current by the following mechanism. When the cell is fully charged and at rest, lithium atoms are stored in the anode at a higher chemical potential than if they were stored in the cathode. The lithium is stored by intercalation within the crystal structure of the anode material. When an electrical circuit is connected between the cathode and the anode, the lithium atoms in the anode split at the anode-electrolyte surface to form Li^+ ions and electrons. The Li^+ ions pass through the electrolyte towards the cathode, whereas the electrons must travel through the anode towards the current collector attached to the anode. The electrons then are conducted through the current collector and around an external circuit which induces an electrical current. The electrons arrive at the opposite current collector, travel into the cathode and reform with Li^+ ions at the cathode-electrolyte surface to form lithium atoms, which are intercalated into the cathode. When the battery is recharged, the induced potential difference causes the lithium atoms to split again at the cathode surface and the opposite process occurs until the lithium atoms are intercalated back into the anode. A simplified schematic of this Li^+ and electron movement when a circuit is attached to an LIB is shown in Figure 1.

The lithium needs to have a lower chemical potential in the cathode than in the anode for the electrons to flow and power to be generated.

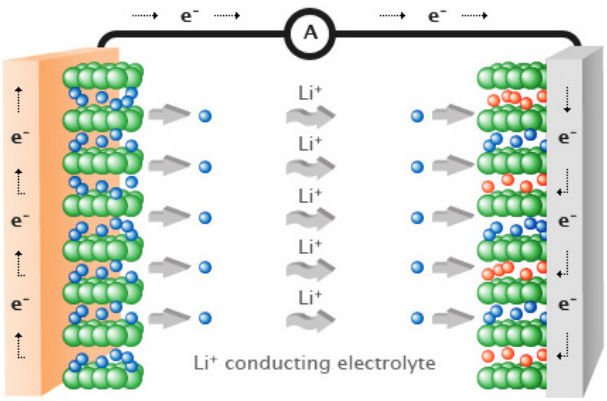

Figure 1 – Schematic of a lithium-ion cell [1].

Two desirable properties of LIBs are high capacity and high power. The capacity of a battery is a measure of how much energy it can deliver from a single charge, which is directly related to the amount of lithium which can be stored within the anode. Typically, this is measured per unit volume (volumetric capacity) or per unit mass (gravimetric capacity). A high volumetric capacity and gravimetric capacity make LIBs ideal for use in portable electronic devices such as laptops, mobile phones and electric vehicles. For a given anode and cathode, the power that battery can deliver is determined by how quickly the electrons move through the external circuit, known as the current. This is determined by the speed of the reactions at the electrode-electrolyte (anode-electrolyte and cathode-electrolyte) surfaces. This is limited by the slow diffusion of lithium atoms through the anode and cathode and thus to increase the power, porosity is often incorporated into the anode and cathode, as seen in Figure 2. The lithium atoms intercalated in the anode has a far shorter distance to diffuse before the reaction at the surface can take place, speeding up this reaction. The lithium ions diffuse through the electrolyte surrounding the electrode particles and react at the surface of a cathode particle to form lithium atoms intercalated in the cathode.

A good lithium-ion battery has high capacity (how much energy can be stored in one charge) and high power (how quickly the energy can be provided).

Silicon Anodes

Silicon has an extremely large capacity for lithium (both volumetric and gravimetric) compared to other common anode materials. This is the reason that Nexeon seeks to include silicon into the anode materials they produce. When fully lithiated, silicon can

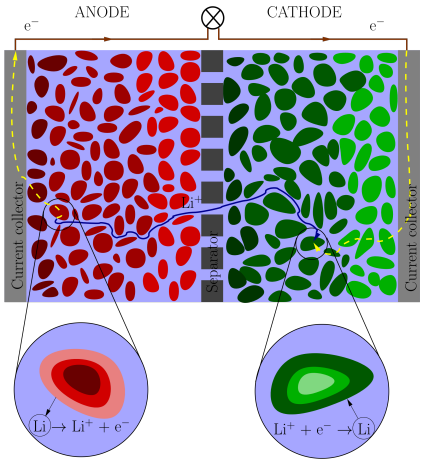

Figure 2 – Schematic of a lithium-ion cell with porous electrodes. There is a separator between the anode and cathode to avoid short-circuiting the battery. The reactions at the anode-electrolyte and cathode-electrolyte surfaces are shown in the circles.

accommodate 3.75 lithium atoms per silicon atom, forming the alloy $Li_{3.75}Si$ at room temperature. This is a very large improvement over the commonly-used graphite which can accommodate one lithium atom per six carbon atoms (0.167 lithium atoms per carbon atom) when it forms the alloy LiC_6. The gravimetric capacities for silicon, graphite and other common anode materials are given in Table 1.

Silicon has an extremely large capacity for lithium but expands significantly when charged, causing mechanical stresses.

	Si	C_6	$Li_4Ti_5O_{12}$	Sn	SnO_2	Ge
Grav. Cap. ($mAhg^{-1}$)	3500	372	175	994	790	963
Volume Change (%)	280	10	1	260	240	270

Table 1 – Gravimetric capacities and volume changes of anode materials.

However, silicon has a significant limitation to its use as an anode material. When fully lithiated, silicon expands to nearly 400% its original volume due to the changes in the crystal structure that occur to accommodate the lithium atoms. This can cause mechanical stresses because of geometrical constraints within the anode and the rest of the battery, but also because of concentration gradients of lithium within the anode itself causing non-uniform expansion. The expansion of the anode can displace other components of the battery, resulting in loss of connection within the cell. Additionally, the high stresses within the anode material may cause it to crack. This loss of connection can lead to parts of the anode being electrically disconnected, which reduces the capacity of the battery over time, commonly known as capacity fade.

Experimental efforts to make silicon a viable anode material have involved using nano-structures within the anode design. These small structures decrease the diffusion length of the lithium into the anode, decreasing the gradients in the lithium concentration and thus decreasing the internal stresses caused by the non-uniform expansion. Some examples of nanoscale designs are nano-particles, nano-wires and nano-tubes. Additionally, there are many nano-scale designs which attempt to constrain the expansion of the silicon, for example in a core–shell structure, yolk–shell structure, or using self-healing polymers. We present SEM images and diagrams of some of these designs in Figure 3 and a review of the developments of silicon-based anode designs is given by Zuo *et al.* [2].

Project Aims

In this project, we focus on modelling the mechanical effects of lithiating an anode and ideally would model the entire porous anode, as shown in Figure 2. However, we choose to model a single anode particle, approximated to be spherical, to gain analytical insight into the stresses and displacement within each anode particle. We also investigate the effect of

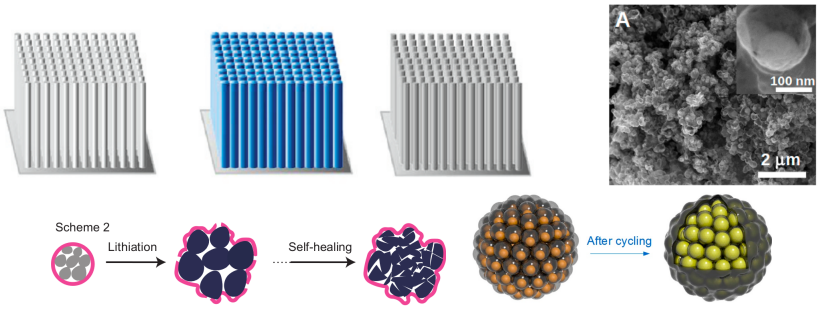

Figure 3 – Schematics and SEM images of experimentally made nano-structured anode designs. Top left: Silicon nano-tubes [3], top right: Yolk–shell design [4], bottom left: Self-healing polymer cages [5], bottom right: Pomegranate structure [6].

mechanical stresses on anode particles comprising two chemically-active materials and use a silicon core surrounded by a graphite shell as an example. The overall aim of the models derived in the project is to improve the design of core–shell anode particles according to the expansion, stress and capacity of the particle.

Glossary of terms

- **Anode particle:** A small particle of anode material used in a porous anode as in Figure 2.
- **Stress:** The internal mecahnical forces experienced by a body.
- **Capacity:** The amount of energy an anode can provide in a single charge.
- **Linear elasticity model:** Mechanical model which assumes the displacements and elastic stresses are small and that the stress–strain relationship is linear.
- **Open-circuit voltage (OCV):** The difference in electrical potential between an anode and cathode when disconnected from any circuit which is a function of lithiation. An anode's OCV is measured against a lithium metal cathode as standard.
- **State of Charge (SOC):** The amount of lithium intercalated into the anode particle, relative to the maximum amount of lithium that could be intercalated.

2 Linear Elasticity Model

In this section, we describe the simple linear elasticity model, coupled to an equilibrium chemical model, which we use to make simple approximations about how the size of the silicon core affects the expansion, stress and capacity of the anode particle.

Anode Particle Geometry

The radius and volume of the silicon core, R_{Si} and V_{Si}, respectively, are measured relative to the radius and volume of the entire anode particle.

Throughout this section, we consider the anode particle to consist of a silicon core and a graphite shell. We denote the radius of the silicon core as R^*_{Si} and the radius of the entire anode particle as R^*_{C}. We denote the ratio of the silicon core radius to the anode particle radius as $R_{\text{Si}} = R^*_{\text{Si}}/R^*_{\text{C}}$ and the ratio of the volume of the silicon core to the volume of the entire anode particle as

$$V_{\text{Si}} = R^3_{\text{Si}} = \frac{\frac{4\pi}{3}(R^*_{\text{Si}})^3}{\frac{4\pi}{3}(R^*_{\text{C}})^3}. \tag{1}$$

A two-dimensional slice through the spherical anode particle is shown in Figure 4.

Description of Model

To simplify the model, we are considering the particle to be in equilibrium and ignoring any transport of lithium through the anode particle. This assumption is valid when charging very slowly or for particles so small that as the lithium is intercalated at the surface, the lithium can diffuse quickly enough throughout the particle to ensure the

chemical potential is uniform. The particle is therefore assumed to be in both mechanical and chemical equilibrium.

In the absence of any mechanical stress, the chemical potential of the intercalated lithium is solely dependent on the anode material and the concentration of lithium in the anode material (state of charge). The stress-free chemical potential can be calculated as a function of the relative concentration of lithium using the open-circuit voltage (OCV), a measure of the difference between the electrochemical potential of the electrons in the anode and that in a reference electrode (usually lithium metal). The stress-free chemical potential of lithium intercalated into silicon and graphite against the state of charge (SOC) is given in Figure 5.

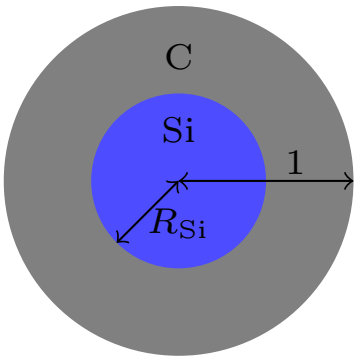

Figure 4 – Two-dimensional slice through spherical anode particle comprising a silicon core of radius R_{Si} relative to the radius of the entire anode particle, denoted by "Si", and a graphite core denoted by "C".

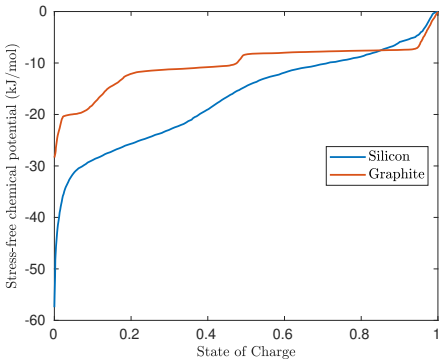

Figure 5 – Stress-free chemical potential of intercalated lithium against relative concentration of lithium within the anode. Adapted from [7] (silicon) and [8] (graphite).

The full chemical potential of the lithium is the sum of the stress-independent chemical potential (determined from the OCV), and the stress-dependent chemical potential.

We also consider a phenomenon known as stress-assisted diffusion in this model. This effect incorporates the contribution of the elastic energy of the anode material into the chemical potential of the intercalated lithium. Therefore, the mechanical stress induced in an expanding anode affects the concentration of lithium intercalated into the anode. If the anode is under compressive stress, the anode is able to intercalate less lithium than if it were stress-free. If the anode is under tensile stress, the anode can intercalate more lithium than if it were stress-free. We assume that the displacement and stress are caused by the intercalation of the lithium causing the anode materials to expand. The intercalation of the lithium is in turn affected by the stresses induced in the anode materials. Therefore, there is a two-way coupling between the mechanical model and the chemical model.

Finally, we assume that the mechanical stiffness of the anode materials depends on the lithiation of the material. For silicon, the stiffness decreases with lithium concentration, whereas for graphite, the stiffness increases with lithium concentration [9].

Chemical Results

How much the materials are being squeezed or stretched (hydrostatic stress), and thus the lithium concentration, is independent of the radial distance from the centre.

One key result of this simple linear, equilibrium model is that the lithium concentration is uniform in each anode material. This is because the hydrostatic stress is independent of the radial distance from the centre of the particle; it only depends on the stiffness of the anode materials, the size of the silicon core, and the expansion of each material. Therefore, the lithium concentrations, which only depends on the anode materials and the hydrostatic stress, are also independent of the radial position in each material and thus are scalar quantities. We label these scalar lithium concentrations in the silicon and graphite as c_{Si} and c_{C}, respectively, and these are relative to the maximum concentration each material can accommodate.

We can calculate the concentration in each material for a given size of silicon core and a given amount of lithium intercalated into the anode particle by equating the chemical potentials of the silicon and graphite as the anode particle is in equilibrium. We measure the amount of lithium intercalated into the anode particle using the SOC. We define the SOC for a multi-material anode as the amount of lithium in the entire anode particle (both

silicon and graphite) relative to the maximum amount of lithium that that particle can accommodate. We plot c_{Si} and c_C against the SOC for anode particles with several different relative volumes of silicon core (labelled as V_{Si}) in Figure 6. For states of charge less than approximately 0.05, c_{Si} increases a small amount and c_C does not increase very much with SOC. Then, the lithium concentration in the graphite increases very rapidly with the SOC and then is saturated ($c_C = 1$) for higher SOC values. The concentration in the silicon, c_{Si}, remains small after its initial increase and only increases rapidly with SOC again once the graphite is saturated. This is because the graphite is stretched a lot by the silicon even when the silicon is only slightly lithiated due to its high expansion. Due to stress-assisted diffusion, the graphite can accommodate much more lithium due to this stretching and thus c_C increases rapidly with SOC. The silicon is being compressed by the graphite shell and thus cannot accommodate as much lithium. However, when the graphite is saturated and the SOC is increased, the lithium must be intercalated somewhere, and thus it is intercalated into the silicon, and c_{Si} increases more rapidly with SOC.

The graphite shell is completely lithiated at low states of charge due to the silicon stretching it by expanding.

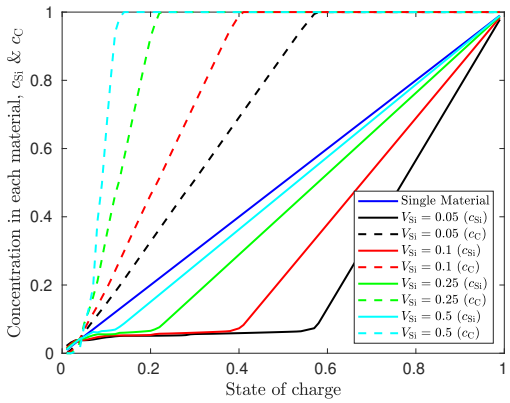

Figure 6 – Relative lithium concentrations against state of charge for several volumes of silicon core.

In our model, we assumed the chemical potential of the intercalated lithium is equal in both materials. We calculate the chemical potential of the intercalated lithium for a given volume of silicon core and SOC and plot the results in Figure 7. We can see that the chemical potential is comparable to the stress-free single-material chemical potentials while the graphite is not saturated, and then increases very rapidly with SOC for higher SOC values. However, even for lower SOC values than that at which graphite is saturated, the chemical potential is higher than both of the single-material chemical potentials. The large increase in the chemical potential at high SOC values is due to the silicon being under compression from the graphite shell, meaning the chemical potential of the lithium intercalated into the silicon is higher than if the silicon was stress-free. However, because the graphite is saturated, increasing the SOC further increases c_{Si} which increases the

The chemical potential of the core–shell particle is very different to that of the individual materials.

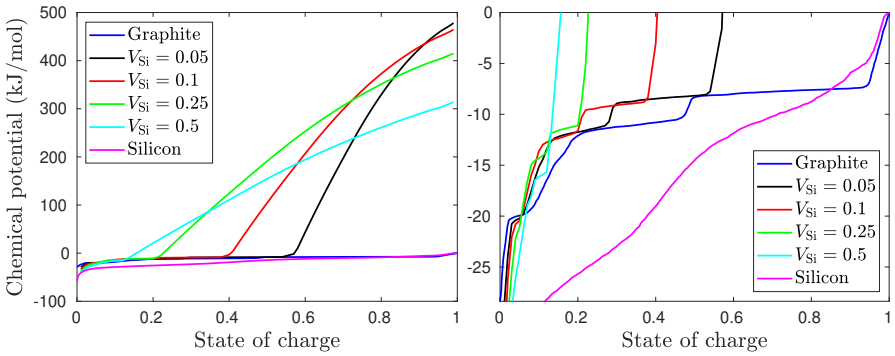

Figure 7 – Chemical potential of the anode particle against state of charge for several volumes of silicon core. The stress-free chemical potentials for silicon and graphite are also plotted. The right-hand figure is focused on the range of chemical potentials seen in the stress-free chemical potentials of silicon and graphite.

amount that the silicon core expands, which increases the compressive stress in the silicon, culminating in a massive increase in the chemical potential of the lithium within.

This simple model could be used to predict open-circuit voltages of multi-material anodes.

By reversing the process of converting the OCVs of silicon and graphite to the stress-free chemical potentials shown in Figure 5, this procedure can be used to predict the OCV of multi-material anode particles. This is potentially very valuable to anode manufacturers as carrying out OCV measurements is very expensive and time-consuming and being able to predict the OCV of a new combination of materials within an anode particle could help reduce these costs. However, this simple model does not take into account any cracking of the materials, or any other damage mechanics, which will most likely occur at the high stresses occurring in the anode particle before reaching the high SOC values used in this example.

Optimal Volume of Silicon Core

We now use this model to gain insight into the optimal volume of silicon core. We wish to find the optimal volume according to three different objectives based on three measures:

- **Relative capacity**: the amount of lithium intercalated into the particle, which will depend on the SOC and the volume of the silicon core, relative to the amount of lithium intercalated into a fully lithiated particle made solely of silicon.
- **Relative expanded volume**: the volume of the anode particle after intercalation at a particular SOC, compared to the volume of the unlithiated particle.
- **Interfacial stress**: the von Mises stress at the interface between the graphite shell and the silicon core. It can be shown that this is the radius of the particle at which the von Mises stress is at its maximum.

From this simple model, we can easily derive measures of success for the anode particle and use these to optimise the volume of the silicon core.

Using these three measures, we define the objectives we will use to optimise the volume of the silicon core:

- **Relative volumetric capacity**: the relative capacity per relative expanded volume.
- **Maximum capacity according to expansion constraint**: the maximum capacity the anode particle can accommodate while keeping the relative expanded volume less than some constraint.
- **Maximum capacity according to expansion constraint**: the maximum capacity the anode particle can accommodate while keeping the maximum induced stress less than some constraint.

In Figure 8, we plot the relative volumetric capacity against the volume of the silicon core. We can see that the optimal SOC is a fully lithiated anode particle, as this would maximise the amount of lithium without increasing the expansion by too much. However, the optimal size of the silicon core can be seen to be around 0.75, as the expansion becomes so large for larger silicon cores that this objective begins to decrease.

In Figure 9, we plot the maximum capacity that can be achieved for several different constraints on the relative expanded volume. We can see there are two regimes to these plots, the linear part for small silicon core volumes and the nonlinear part for larger cores. The linear regime is caused by silicon core sizes which have an expanded volume less than the constraint even at full lithiation. Anode particle designs corresponding to the nonlinear part must have a restricted lithiation (SOC < 1) to ensure the expanded volume does not exceed the constraint. We can therefore see that the optimal volume of silicon core is that which has an expanded volume equal to the constraint when it is fully lithiated. This design corresponds to the peaks between the linear and nonlinear regimes.

Finally, we plot the maximum capacity under several interfacial stress constraints against the silcon core volume in Figure 10. We can see that for all the constraints, the optimal design is as large a silicon core as possible. However, for larger constraints, there are local minima and maxima. Therefore, if this optimisation is used in conjunction with other constraints, these local maxima may be the optimal designs. Graphite will mechanically fail at stresses much less than the constraints shown here, and so to maximise the capacity such that the graphite does not fail, a large silicon core with a very low state of charge would be optimal. Of course, if there was no graphite shell at all, the interfacial stress would be zero and this would be the optimal for this objective.

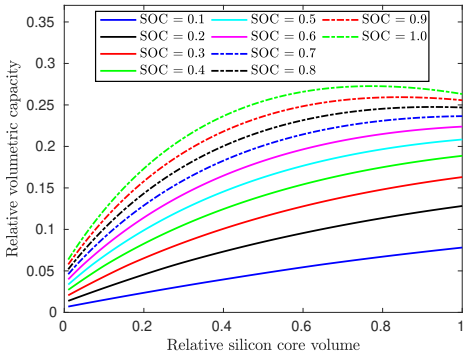

Figure 8 – Relative volumetric capacity against the relative volume of silicon core, V_{Si}.

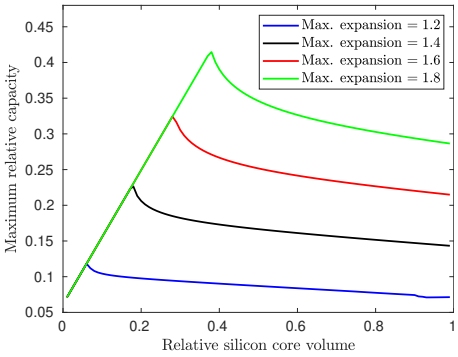

Figure 9 – Maximum capacity against volume of silicon core, V_{Si}, for several different expansion constraints.

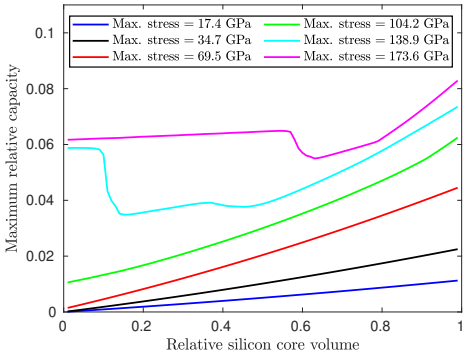

Figure 10 – Maximum capacity against volume of silicon core, V_{Si}, for several different interfacial stress constraints.

3 Porosity

We now investigate whether the use of porous silicon within the anode particle design in Figure 4 can reduce the expanded volume of the lithiated anode particle without sacrificing the capacity of the anode. The structure of the porous silicon we consider is shown in Figure 11. The porous structure is made up of a repeating unit shown in the right-hand side of Figure 11. The reason we use this structure is so we can exploit the periodicity within the structure to obtain effective parameters, such as stiffness and the amount the porous silicon expands, at a low computational cost using the method of multiple scales [10]. These effective parameters can then be used within the simple model in Section 2 as if the porous silicon was made of one homogeneous material.

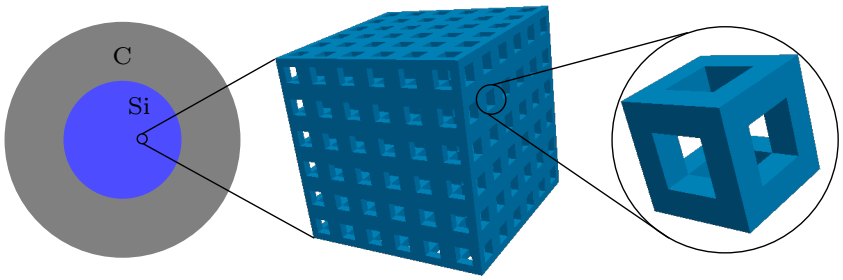

Figure 11 – Diagram of the structure of the porous silicon.

We utilise the porous silicon in two ways: replacing the non-porous silicon core with a porous one, and incorporating a porous silicon layer between the non-porous silicon core and the graphite shell. These two structures are shown in Figure 12. Instead of finding

We investigate using porous silicon to weaken the silicon so that the graphite shell can hopefully constrain it more easily but the high capacity of silicon is retained.

the optimal volume of silicon core and SOC as in Section 2, we now attempt to reduce the relative expanded volume of the anode particle (defined in Section 2) without sacrificing the capacity. We do this by comparing the relative expanded volume at full lithiation of anode particle designs with porous silicon with those with only a non-porous silicon core but with the same capacity. The size of the porous silicon core will therefore have to be larger than the non-porous counterpart as the porous silicon cannot accommodate as much lithium due to the pores.

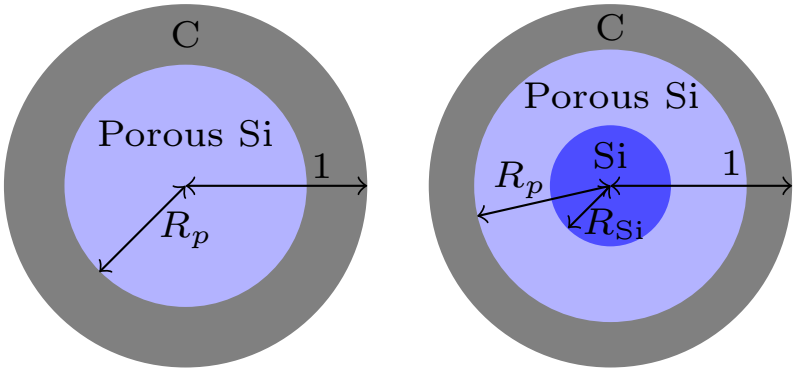

Figure 12 – Two-dimensional slices through each of the anode particles incorporating porous silicon into them. Similar to Figure 4, we label the outer radius of each layer relative to the outer radius of the anode particle and use R_p to label the outer radius of the porous silicon regions.

Porous Silicon Results

In Figure 13, we plot the relative expanded volume at full lithiation against the relative capacity of the anode particle at full lithiation for different volume fractions of silicon in the porous silicon core design in the left diagram of Figure 12. The capacity is varied by varying the volume of the porous silicon core and the lower the volume fraction, the more porous the silicon core. As porous silicon can accommodate less lithium than non-porous, the maximum capacity of the porous silicon core designs is lower than for the non-porous designs. The right-hand figure shows that there are certain sizes of silicon core that have a lower expanded volume than a particle with a non-porous core with the same capacity.

In Figure 14, we plot the relative expanded volume at full lithiation against the relative capacity of the anode particle at full lithiation for different volume fractions of silicon in the porous silicon layer in the right diagram of Figure 12. In each of the figures in Figure 14, the ratio between the outer radius of the silicon core (R_{Si}) and that of the porous layer (R_p) is held constant. It can be seen that for both plots in Figure 14, there are anode particle

The model shows that certain anode particle designs which use porous silicon can reduce the expansion of the particle if only non-porous silicon was used, without sacrificing the capacity.

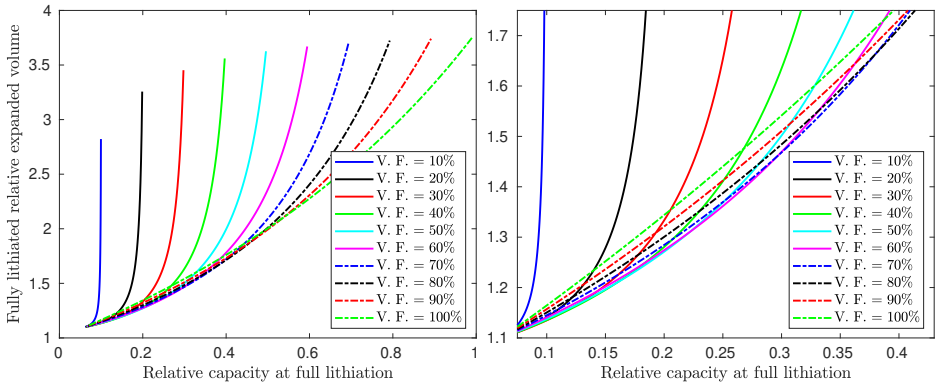

Figure 13 – Fully lithiated relative expanded volume against relative capacity at full lithiation for several different volume fractions (V. F.). The right-hand figure is focused on the range of capacities which a porous core can reduce the expansion compared to a non-porous core (V. F. = 100%) without sacrificing the capacity.

We compare the expansion of anode particle designs with the same capacity, not with the same volume of silicon core.

designs with porous layers which can reduce the expanded volume without sacrificing the capacity of the particle. Furthermore, in the case of the right plot, the reduction in expanded volume is fairly large for some volumes of silicon core.

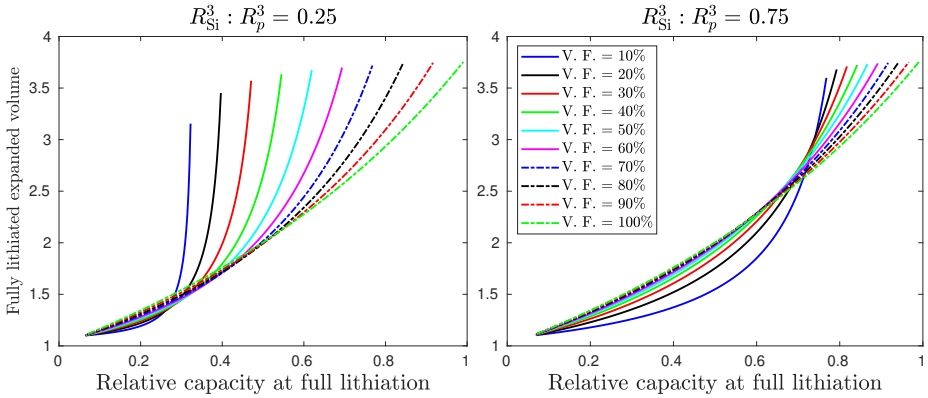

Figure 14 – Fully lithiated relative expanded volume against relative capacity at full lithiation for several different volume fractions (V. F.). In each figure, the ratio between the outer radius of the non-porous silicon core (R_{Si}) and the outer radius of the outer radius of the porous layer (R_p) is held constant. The legend for the left figure is the same as the right.

The linear model produces unphysical results, but a nonlinear model shows that some specific designs can also achieve a slightly lower expansion without sacrificing the large capacity of silicon.

These results are promising for the use of porous layers in anode particles. However, if the results of designs with very porous and thin porous silicon layers are analysed more closely, we can see that the large reduction in expansion seen in the Figure 14 is due to the model showing that the non-porous silicon core and the porous silicon layer overlap when expanded. This is clearly unphysical and is due to a break down of the linear elasticity model in this case.

Nonlinear Elasticity Model

A nonlinear elasticity model was adapted from [11] to attempt to fix the overlap seen in the results from Section 3 by allowing large deformations. For a non-porous silicon core and a grahite shell, however, the model was shown to not yield mathematical solutions for certain silicon core volumes and states of charge. However, when the stress–strain law was changed to also be nonlinear, solutions for the porous silicon layer designs could be found without overlap. These results show that reduction in the expanded volume without reduction in capacity could still be achieved for certain designs with a porous silicon layer. However, the constitutive laws used in this nonlinear model do not accurately describe silicon or graphite so the validity of these results is unclear.

4 Damage Model

We model the graphite as being pulverised if it is subject to a certain amount of stress from the silicon. This pulverised graphite is modelled differently to the non-pulverised graphite.

If the stress in the graphite shell becomes too great, the graphite shell will crack or mechanically yield, causing the anode particle to fail. We model this by using the linear elasticity model from Section 2 but assuming the graphite becomes pulverised if the stress in the graphite shell exceeds its yield stress. We use the von Mises stress as the scalar measure for the stress and this is non-uniform in the graphite shell. Therefore the graphite shell may be partially pulverised up to a certain radius — the maximum von Mises stress can be shown to be at the core–shell interface — and is still intact at greater radii. We label the radius up to which the graphite is pulverised, relative to the radius of the entire anode particle, as R_{pulv}, as shown in Figure 15.

We plot the outer radius of the pulverised graphite against the SOC in Figure 16. As the SOC increases, the silicon expands more, increasing the stress in the graphite and so more of the graphite exceeds the yield stress so the pulverised graphite region grows. The pulverised graphite region grows rapidly for very low states of charge until eventually the entire graphite shell is pulverised ($R_{pulv} = 1$) at still low states of charge. This is due to the yield stress of graphite being very low compared to the stresses that the expanding silicon core induces in the graphite.

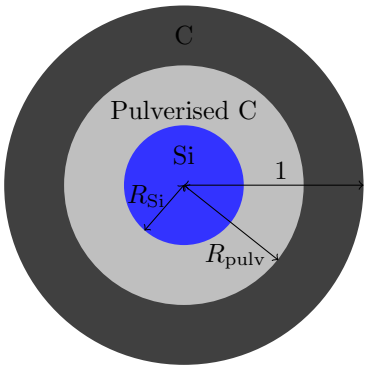

Figure 15 – Anode particle with silicon core and partially pulverised graphite shell.

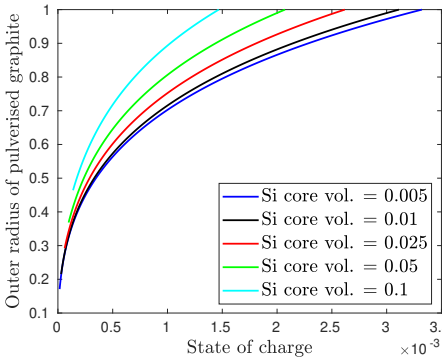

Figure 16 – Position of pulverised front against the SOC.

If the whole of the graphite shell becomes pulverised, the shell will fail completely and will cease to constrain the silicon. This will also lead to damage to the silicon core due to contact with the electrolyte. We plot the relative capacity at the SOC that the graphite fully pulverises against the relative silicon core volume in Figure 17. The largest capacity that can be achieved while the graphite is not yet fully pulverised is using as large a silicon core as possible. However, the capacity is still very low as the lithium concentration must remain extremely low to avoid fully pulverising the graphite.

Finally, to assess the viability of a fully lithiated anode particle, we plot the relative outer radius of the pulverised graphite when the anode particle is fully lithiated against the relative silicon core volume in Figure 18. This model shows that the silicon core volume relative to the entire anode particle must be less than approximately 6.5×10^{-5} to avoid fully pulverising the graphite shell. This implies that only a tiny amount of silicon can be added to the anode particle to avoid the graphite from completely pulverising if the anode is to be fully charged. This is due to the very small yield stress of graphite compared to the stresses induced by the silicon.

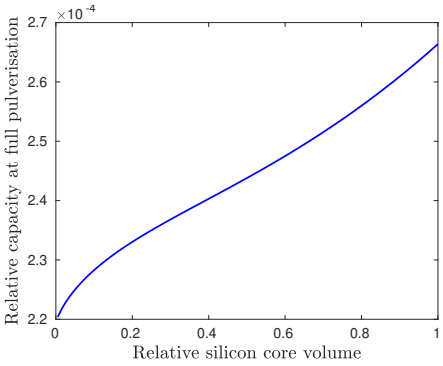

Figure 17 – Relative capacity when the graphite is fully pulverised against relative silicon core volume.

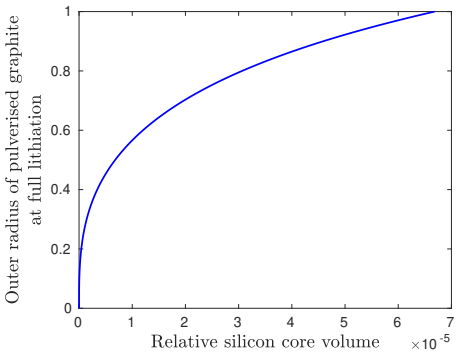

Figure 18 – Outer radius of pulverised graphite at fully lithiation against relative silicon core volume.

5 Discussion and Recommendations

We have modelled the mechanical impact of lithiating a spherical anode particle comprising a silicon core and a graphite shell. We showed in Section 2 that even when charging slowly, the stress induced by each anode material on the other has a large effect on the distribution of lithium within the particle and on the chemical potential of the lithium. Using three different objectives, we optimised the volume of the silicon core. According to the simple linear model:

- A silicon core around 0.75 the volume of the entire anode particle maximises the volumetric capacity.

- If a volumetric constraint is imposed, a particle with a silicon core which expands to this constraint at full lithiation will maximise the capacity whilst remaining below the expansion constraint.
- A large silicon core will maximise the capacity subject to interfacial stress constraints, but there are other local optima.

In Section 3 we saw that using a porous silicon core or a porous silicon layer between the core and the shell can reduce the expansion without sacrificing the capacity. However, for some extreme designs, this simple model produces unphysical results. In Section 4 we included the pulverisation of the graphite at high stress, and analysed how the pulverised region grows with the SOC when charging the particle. We saw that if the particle is to be fully lithiated, only a tiny silicon core can be used without fully pulverising the graphite.

From the results in this report, there are three key outcomes to be made:

- This model can be used to approximate an effective OCV for core–shell anode particles using the OCVs of the original materials and the stress induced.
- Using porous silicon could reduce the expansion of an anode while keeping the increased capacity caused by the silicon.
- Even a tiny silicon core could cause severe damage to the graphite shell, potentially causing severe capacity fade.

This model makes several assumptions that are not applicable to normal battery usage, however. For example, the equilibrium assumption is only applicable for extremely slow charging, or extremely small anode particles. Also, in the models before Section 4, the anode materials will change behaviour when the stress becomes very high and this is not considered. Instead, this simplified model is useful for gaining analytical insight and understanding into the expansion and stresses within core–shell anode particles which can be used to aid particle design.

6 Impact

"Nexeon has valued the insights gained from the work that Ian Roper has undertaken during his research project Silicon anodes in lithium batteries and his earlier mini project. These mathematical studies have complemented the work on silicon containing battery anode materials conducted by Nexeon. In addition to the direct interactions with Ian during his project there have been valuable discussions with both Colin and Jon at regular intervals and the wider networking with the InFoMM team."

- Bill Macklin, Industrial Supervisor, Nexeon

References

[1] Nexeon. Nexeon - About Li-ion batteries: `www.nexeon.co.uk/technology-2/about-li-ion-batteries`, Accessed on 18/07/2017.

[2] X. Zuo, J. Zhu, P. Müller-Buschbaum, and Y. Cheng. Silicon based lithium-ion battery anodes: A chronicle perspective review. *Nano Energy*, 31:113–143, 2017.

[3] T. Song, J. Xia, J. H. Lee, D. H. Lee, M. S. Kwon, J. M. Choi, J. Wu, S. K. Doo, H. Chang, W. I. Park, D. S. Zang, H. Kim, Y. Huang, K. C. Hwang, J. A. Rogers, and U. Paik. Arrays of sealed silicon nanotubes as anodes for lithium-ion batteries. *Nano Letters*, 10(5):1710–1716, 2010. ISSN 15306984. doi: 10.1021/nl100086e.

[4] N. Liu, H. Wu, M. T. McDowell, Y. Yao, C. M. Wang, and Y. Cui. A yolk–shell design for stabilized and scalable Li-ion battery alloy anodes. *Nano Letters*, 12(6):3315–3321, 2012. doi: Doi10.1021/Nl3014814. URL `http://pubs.acs.org/doi/pdfplus/10.1021/nl3014814`.

[5] C. Wang, H. Wu, Z. Chen, M. T. McDowell, Y. Cui, and Z. Bao. Self-healing chemistry enables the stable operation of silicon microparticle anodes for high-energy lithium-ion batteries. *Nature Chemistry*, 5(12):1042–8, 2013. ISSN 1755-4349. doi: 10.1038/nchem.1802. URL `http://www.ncbi.nlm.nih.gov/pubmed/24256869`.

[6] N. Liu, Z. Lu, J. Zhao, M. T. McDowell, H. Lee, W. Zhao, and Y. Cui. A pomegranate-inspired nanoscale design for large-volume-change lithium battery anodes. *Nature Nanotechnology*, 9(3):187–192, 2014.

[7] J. Li and J. R. Dahn. An in situ X-ray diffraction study of the reaction of Li with crystalline Si. *Journal of The Electrochemical Society*, 154(3):A156–A161, 2007.

[8] Y. Reynier, R. Yazami, and B. Fultz. The entropy and enthalpy of lithium intercalation into graphite. *Journal of Power Sources*, 119-121:850–855, 2003. ISSN 03787753. doi: 10.1016/S0378-7753(03)00285-4.

[9] Y. Qi, L. G. Hector, C. James, and K. J. Kim. Lithium concentration dependent elastic properties of battery electrode materials from first principles calculations. *Journal of The Electrochemical Society*, 161(11):F3010–F3018, 2014.

[10] R. Burridge and J. B. Keller. Poroelasticity equations derived from microstructure. *The Journal of the Acoustical Society of America*, 70(4):1140–1146, 1981.

[11] Z. Cui, F. Gao, and J. Qu. A finite deformation stress-dependent chemical potential and its applications to lithium-ion batteries. *Journal of the Mechanics and Physics of Solids*, 60(7):1280–1295, 2012.